Pretargeted Immunoscintigraphy: Effect of Hapten Valency on Murine Tumor Uptake

David A. Goodwin, Claude F. Meares, Maureen McTigue, Warak Chaovapong, Carol I. Diamanti, Charles H. Ransone and Michael J. McCall

Nuclear Medicine Service, Veterans Administration Medical Center, Palo Alto, California; Stanford University School of Medicine, Stanford, California and Department of Chemistry, University of California, Davis, California

A method of radioimmunoscintigraphy using bivalent "Janus" haptens with an apparent enhanced affinity ("avidity") for the antibody is described. Janus with 50 μg pretargeted Mab WC3A11 resulted in significantly higher murine tumor concentrations (~7%/g) compared to monovalent haptens (~1.4%/g, $p < 0.001$), and the same high tumor-to-background ratios (~3/1). Janus was synthesized by coupling two molecules of BABE together with a 1,4 butanedithiol linker. Janus itself was rapidly excreted ($T_{1/2_b}$ = 42 min) by the kidneys and did not concentrate in any other organs or tissues. Three-step pretargeted immunoscintigraphy (binder, chaser, tracer) with ^{111}In- or ^{67}Ga-Co(III) Janus produced excellent mouse tumor images in 3 hr with high tumor-to-background ratios. The use of short-lived tracers, such as ^{99m}Tc and ^{68}Ga, with a $T_{½p}$ of hours to image antibodies that localize slowly over several days in vivo is accessible with this new technology.

J Nucl Med 1992; 33:2006–2013

Radioimmunoscintigraphy with chelate conjugates of monoclonal antibodies has produced improved images of human tumors, but high blood and liver background remains a significant problem (*1*). When ^{111}In chelate conjugates of monoclonal antibodies are used, liver background is especially high (*2*). Maximum human tumor concentrations of whole antibody may be achieved in one day, but most investigators suggest waiting at least one to three days, and some even up to nine days for the background to clear, in order to attain acceptable target-to-background ratios (*3*). This prolonged retention of radioactivity not only lowers the target-to-background ratios but also increases the radiation dose to the patient. Effective methods for reducing liver, blood and other nontarget background must be found if the potential of monoclonal antibodies in tumor imaging and therapy is to be fully realized.

We have developed pretargeted immunoscintigraphy with radioactive haptens as one of several possible solutions to this problem (*4,5*). A three-step method was used in which the antibody and the radiolabel were administered separately (*5*). Nonradioactive antibody was given to BALB/c mice bearing KHJJ tumors (pretargeted) and allowed one day to reach maximum tumor concentration (a longer time may be necessary in humans). At the time of maximum tumor concentration of nonradioactive antibody, the blood was quickly cleared of excess circulating nonradioactive antibody with a special intravenous "chase." One hour after the chase, a monovalent radiolabeled hapten-chelate conjugate was given, and images were made in 3 hr. These experiments suggested pretargeting could lead to greatly decreased radiation exposure in patients through rapid renal excretion of the unbound radiolabel and by eliminating the need for long-lived tracers like ^{131}I and ^{111}In currently used for antibody labeling.

We (*6*) and others (*7*) have further suggested that bivalent haptens would improve in vivo binding to pretargeted antibody due to enhanced "functional affinity." This effect has already been demonstrated in other multivalent antigen-antibody binding systems (*8*). Here we present improved results; results with bivalent haptens in a pretargeting strategy in tumor mice. These Janus haptens increased the tumor uptake compared to the original method using monovalent haptens (*5*), but maintained the same high tumor-to-background ratios (*6*).

MATERIALS AND METHODS

Chemistry

HPLC. Analytical high-performance liquid chromatography (HPLC) was performed using two Waters (Milford, MA) 45 pumps controlled by a Waters 660 Solvent Programmer connected to a semi-prep (10 mm × 250 mm) C_{18} column (Alltech Assoc., Deerfield, IL). Purification of Janus was done using a Rainin Rabbit HPLC System and Rainin Dynamax 60-Å preparative (21.4 mm × 250 mm) C_{18} column. The solvent gradient was controlled by MacRabbit software on a Macintosh Plus computer. Both HPLC systems used ISCO (Lincoln, NE) UA-5 Absorbance Monitors connected to ISCO type 6 detectors set at 254 nm wavelength. HPLC analysis used a 20-min linear gradient from 0.1 *M* aqueous sodium acetate (pH 7, containing 1 m*M* EDTA) to 100% methanol while the HPLC purification was the same except that some samples of trifluoroacetate were used

Received Jan. 16, 1992; revision accepted Jun. 1, 1992.

For reprints contact: David A. Goodwin, MD, Professor of Radiology and Nuclear Medicine, Stanford University School of Medicine, Chief of Nuclear Medicine, Veterans Administration Medical Center, 3801 Miranda Ave., Palo Alto, CA 94304.

instead of acetate and there was no EDTA in the aqueous phase. Solvent flow rates were 3 ml/min for analysis and 12.5 ml/min for preparative scale.

NMR. Proton NMR spectra were recorded on a 300 MHz General Electric QE-300. Chemical shifts are reported in ppm relative to HDO (4.75). Mass spectral and exact mass measurements were made on a ZAB-HS-2F mass spectrometer (VG Analytical Instruments). Thin-layer chromatography was done as described previously (*9*).

Synthesis of 1-(p-bromoacetamidobenzyl)-EDTA (BABE). The brominated chelate was synthesized using a variation of the procedure described by Mukkala (*10*). 226.6 mg (0.57 mmole) of (S)-1-p-aminobenzyl-EDTA, prepared as described earlier (*9,11*), was added to 18 ml of H_2O, the pH adjusted to 7.4 using 3 *M* NaOH and then 489 μl of neat diisopropylethylamine added. To the aqueous solution, we added 18 ml of chloroform and then vigorous stirring was applied with a magnetic stir bar before adding 283 μl (3.25 mmole) of bromoacetyl bromide. The reaction was allowed to stir for 30 min at room temperature. After removing the aqueous phase, the organic phase was washed three times with water and then the aqueous phase given three rinses with chloroform. The second and third chloroform rinses were negative to the alkylating group sensitive reagent 4-(p-nitrobenzyl)pyridine (NBP) (*12*). HPLC analysis of the three peaks showed that the major peak, eluting with a retention time of 12′ 45″ and comprising 96% of total peak area, was 4-(p-nitrobenzyl)pyridine positive, but negative to the amine sensitive reagent fluorescamine (*13*). There were two small contaminant peaks: the first eluted at 5′ 12″ and had 0.5% of total peak area, while the second eluted at 12′ with 3% of the peak area. Both contaminant peaks were negative to 4-(p-nitrobenzyl)pyridine and fluorescamine. It has been learned that the desired product will break down into a number of unidentified compounds when stored at room temperature or 4° C in concentrated aqueous solutions, but can be safely frozen in liquid N_2 and stored at −80° C. The product solution was used immediately in the next synthesis step without purification.

Synthesis of Janus. A solution of 1-(p-bromoacetamidobenzyl)-EDTA, 0.125 mmole in 40 ml H_2O as determined by metal binding assay (*9*), was vigorously stirred with a magnetic stir bar before adding 7.3 ml (0.062 mmole) of 1,4 butanedithiol followed by 85 ml of 4 *M* NaOH, which changed the pH from 2.6 to 7.4. The pH was kept between 7.4 and 7.6 during the 1.5-hr reaction time until the solution was negative to both 4-(p-nitrobenzyl)pyridine and the thiol-sensitive Ellman's reagent, 5, 5′-dithiobis(2-nitrobenzoic acid) (*14*). HPLC analysis revealed almost complete conversion of the 1-(p-bromoacetamidobenzyl)-EDTA to the Janus product, with two additional small contaminant peaks eluting at 11′ 12″ (9% of the total peak area) and at 18′ 24″ (3% of total peak area). These two contaminant peaks were negative to fluorescamine, 4-(p-nitrobenzyl)pyridine, and 5, 5′-dithiobis(2-nitrobenzoic acid). To remove the traces of diisopropyl-ethylamine left over from the previous step after HPLC of the major peak, the product was applied to a 125 ml Bio-Rad AG-50 (Na^+) resin column that had been washed with 5 column volumes of 3 *M* NaOH and then equilibrated to pH 7.8 with H_2O. The product quickly eluted in the first column volume of applied H_2O rinse as determined by TLC. The final Janus product concentration was 2.64 m*M* as determined by metal binding assay. The FAB mass spectrum showed a single peak at the expected M+1 of 998: ^1H NMR (D_2O, pH 3.8) 7.50 (d, 4H), 7.35 (d, 4H), 3.96 (d, 5H), 3.85 M, 14H), 3.48 (d, 4H), 3.44 (s, 5H), 3.25 (t, 2H), 2.80 (t, 2H), 2.63 (s, 3H), 1.75 (s, 3H). The product had the expected 8:38 ratio of aromatic to aliphatic protons.

Synthesis of Co(III) Janus. To a solution of 120 mg BABE (0.232 mmole,) in 7.0 ml of water was added 2.4 ml of 100 m*M* cobalt(II) acetate and 30 μl of 30% hydrogen peroxide (ca. 0.294 mmole). Addition of 200 μl of saturated aqueous sodium bicarbonate neutralized the solution and a color change from pink to burgundy was observed. The reaction was incubated at room temperature for 2 hr and then lyophilized. The lyophilization residue was taken up in 1.1 ml of water and applied to a 1 × 27 cm P2 (BioRad) column equilibrated in water. The product was eluted with water, coming off the column as the slowest moving colored band. The product-containing fraction was lyophilized to dryness and the Co(III)-BABE residue was characterized by HPLC (single peak at 14-min retention time) and FAB mass spectrometry (M+1 peaks at 575 and 577 (two Br isotopes)). Yield 56 mg (0.097 mmole; 42%).

A solution of 56 mg Co(III)-BABE in 3 ml of water was added dropwise with stirring to a solution of 1 ml 1,4-butanedithiol, and 1 ml of triethylamine in 25 ml of methanol. The reaction was incubated at room temperature overnight under a slow stream of nitrogen. The reaction was removed from the stream of nitrogen, diluted with 15 ml of water, extracted with chloroform (2 × 5 ml) and lyophilized. The residue was taken up in 10 ml and the product characterized by HPLC (18-min retention time) and TLC (single spot at R_f 0.95 which gave a negative NBP test and a positive DTNB test). Quantitation by DTNB gave the concentration of the 1,4-DT-BABE-Co(III) as 1.8 m*M*: Yield ca. 11 mg (18 μmole, 19%).

A solution of 9.4 mg (18 μmole) BABE was dissolved in 200 μl of 0.1 M sodium phosphate buffer, pH 7 and 100 μl of saturated trisodium phosphate solution was added to raise the pH to approximately 10. This solution was added dropwise to the 1.8 m*M* solution of 1,4-DT-BABE-Co(III). The pH of the resulting solution was 9. The solution was incubated at room temperature, under nitrogen, until testing negative for free thiol groups using DTNB (approximately 1 hr). The product Co(III) Janus was isolated by preparative HPLC (retention time 15.5 min) as one of four peaks in the chromatogram. The product was identified on the basis of metal binding and high resolution FAB mass spectrometry. Molecular weight of $C_{42}N_{54}N_6O_{18}S_2Co$ is 1053.2268 theoretical, 1053.261 found. HPLC of the final preparation showed that the product fraction was contaminated by impurities eluting immediately prior to and immediately after the product peak, but the material was used in the preliminary work without further purification.

Radiolabeling Co(III) Janus. Five nmole of Co(III) Janus in 50 μl of 0.1 *M* ammonium citrate was added to purified, dried ^{111}In chloride in a metal free polyethylene tube. Five to 10 nmole Co(III) Janus in 0.1 *M* HCl was added to purified, dried ^{67}Ga in a similar tube. Twenty-five microliters 0.5 *M* sodium acetate was added to the ^{67}Ga solution to raise the pH above 3.0. Finally 10 nmole calcium disodium EDTA was added to bind any unchelated radioactive metal ions. At each step a 1-μl aliquot was spotted on silica gel 60 thin-layer chromatography strips. The strips were dried in a stream of cool air and developed in a solvent composed of equal volumes of menthanol and 5% (W/V) aqueous ammonium acetate. After the strip was dried in a stream of warm air, it was autoradiographed, cut into segments and counted in a well scintillation counter. Then, ^{111}In and ^{67}Ga

radiolabeling was done in the same way with 5–10 nmole of *metal-free* Janus, followed with a slight molar excess of Co(III) acetate and 30 μl of 30% hydrogen peroxide to give ^{111}In and ^{67}Ga labeled Co(III) Janus. Specific activity ranged from 250–850 Ci/mole making it possible to inject large amounts of activity to obtain images, while keeping the Ab/Janus hapten ratio between 1:1 and 0.3:1. Radioactive impurities were always <10% of the total (Fig. 1).

Synthesis of Transferrin-2-Iminothiolane-BABE Conjugate "Chase." Human transferrin (4.73 mg) was dissolved in 200 μl of 0.1 *M* tetramethylammonium phosphate, pH 8.0 and 170 μl of 9.4 mM BABE solution and 30 μl of 30 m*M* 2-iminothiolane (2-IT) in 50 m*M* triethanolamine, pH 8.5, were added. The pH was adjusted to 7.89 with 8 μl of 2 *M* triethanolamine and the solution was incubated at 37° C for approximately 2.5 hr. Final concentrations of 2-IT and BABE were 2.2 m*M* and 3.9 m*M*, respectively. The conjugate was separated from unreacted BABE and 2-IT and the buffer was changed to 0.1 *M* ammonium citrate, pH 5.5, by spin column gel chromatography (*15*). The concentrations of transferrin and BABE in the spin column effluent were determined by UV absorbance at 280 nm (159 μ*M* transferrin) and by metal binding assay (625 μ*M* BABE) (*9*). The chelate sites were filled with Co(III) as described above.

Monoclonal Antibodies

Using standard hybridoma technology with the antigen KLH-2IT-BABE-Co(III), we generated monoclonal antibodies which bound specifically to Co(III) ½ Janusol and In(III) ½ Janusol (*4*, *5*). BALB/c mice were immunized intraperitoneally with 10 μg of KLH-2IT-BABE-Co(III), in complete Freund's adjuvant. Two weeks later this was repeated in incomplete Freund's adjuvant, followed in a further 2 wk with an i.v. booster dose of the conjugate alone. The mice were screened for antibody production after 1 wk by measuring the 24-hr retention of i.v. ^{57}Co, ^{67}Ga or ^{111}In haptens, by whole body counting with a Picker dual probe scintillation counter. The mice with ~50% retention at 24 hr (compared to ~3% in control nonimmunized mice) were hyperimmunized with 30 μg i.v. conjugate and 3 days later their spleen cells were fused with PX63 AG8 myeloma cells. Hybridomas were selected in HAT medium. Clones obtained were screened by ELISA using human transferrin-2IT-BABE-Co(III) as the solid phase antigen coated on μtiter plates. Positive clones were recloned by limiting dilution and five high titer secretors including WC3A11 (IgG1), Ga1A7 and Ga2H1 were selected. These hybridomas were grown in ascites fluid and purified by ammonium sulfate precipitation twice. Protein concentration was determined both by Lowry's method (*16*), and by 280 nm absorbance. The antibody concentration was ~80% of the total protein as judged by gel electrophoresis.

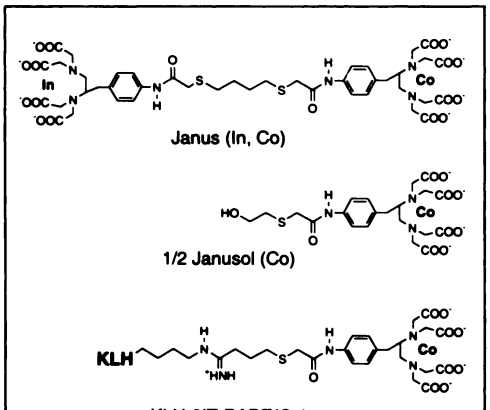

FIGURE 1. (Top) The bivalent hapten Janus, is two bromoacetamidobenzyl-EDTA derivatives linked together with 1, 4 dithiol butane. When radiolabeled with carrier-free ^{111}In, most of the Janus which is in great excess will contain ^{111}In in one site only. Cobalt can then be added afterward to produce the double labeled structure shown above. (Middle) Monovalent ½ Janusol is half the Janus molecule with an ethanol on the sulfur group. (Bottom) The KLH-2IT-BABE-Co(III) conjugate used to immunize the mice.

Antibody Affinity Measurements

The affinity constant (K_A) of WC3A11 was measured by equilibrium dialysis in triplicate for monovalent ^{57}Co-Co(III) and ^{111}In-In(III) ½ Janusol as well as bivalent ^{57}Co-Co(III) and ^{111}In-In(III) Janus. The concentration of WC3A11 was 10^{-7}–10^{-8} *M*; or approximately the reciprocal of the expected K_A. The hapten/antibody binding site concentration ratios spanned the range from 0.01–1.0, so that at least one half of the antibody combining sites were bound to hapten. The large amount of data was analyzed using the Microsoft Excel® spreadsheet to generate Scatchard plots. The least squares mean fit programs Linest and Trend (Microsoft Excel Function Reference 1990, 1991: 138 and 238) were used to obtain the slope and correlation coefficient r^2. The mean K_A of six such experiments for each hapten antigen was calculated and this value plus or minus the s.d. recorded.

Biological Half-life

The complex of 50–600 μg (0.33–3.96 nmole) WC3A11 premixed with 30 μCi (~0.1 nmole) ^{111}In-, ^{67}Ga- or ^{57}Co-labeled Co(III) Janus, was given i.v. to normal BALB/c mice. The ^{111}In-Co(III) Janus was studied alone in four control mice, or mixed with WC3A11 in 21 mice. The ^{67}Ga-Co(III) Janus (seven mice), and ^{57}Co-Co(III) Janus (four mice) were also studied with appropriate controls. The disappearance half-life was measured by whole body counting in a dual probe scintillation system. Animals pretargeted 21 hr earlier with 50 (0.33 nmole) Mab were also studied after i.v. tracer hapten.

Organ Distribution

Tumor and organ assay was done 24 hr after injection of 50 μg (0.33 nmole) Mab i.v. in BALB/c mice with KHJJ tumors (n = 3 per group) (*17*). Antibody was followed in 20 hr by 2 to 4 nmole (~50–100 μg) of chase i.v. Chase compounds were conjugates of chelates with human transferrin, synthesized to contain at least three to four molecules of covalently coupled hapten [2 IT BABE-Co(III)] per molecule of human transferrin. This permitted cross-linking and lattice formation with antibody to occur rapidly in vivo. One hour later (at 21 hr postantibody), 3 μCi (~0.01 nmole) ^{111}In- or ^{67}Ga-labeled Co(III) Janus was administered i.v. The animals were sacrificed 3 hr after administration of tracer (at 24-hr postantibody), and labeled hapten concentrations determined in blood, heart, lungs, liver, spleen, kidneys, tumor, muscle, bone + marrow (femur), skin and gut. In control experiments, either the chase or the pretargeted antibody was omitted (n = 3 per group).

Mouse Imaging

Whole body pinhole gamma camera images of BALB/c mice with KHJJ tumors in the flank were made immediately and 3 hr

after ^{111}In-Co(III) Janus or ^{67}Ga-Co(III) Janus intravenous injection. The mice were sedated with chloral hydrate and 200k count gamma camera images obtained with the pinhole 3 in. above the dorsum of the mouse. The percent remaining in the whole mouse was calculated from the decay-corrected 3-hr counts expressed as a fraction of the whole body counts obtained immediately after injection. The percent in the tumor was obtained from tumor ROI counts.

These tumor mice were pretargeted with 50 μg (0.33 nmole) of WC3A11 intravenously. This was followed in 20 hr with 100 μg of transferrin Co(III) 2IT-BABE chase intravenously. One hour was allowed for the chase to clear the blood of antibody before injecting 100–500 μCi (0.3–1.0 nmole) of either ^{111}In-Co(III) Janus (five mice) or ^{67}Ga-Co(III) Janus (four mice). In control experiments, either the chase [^{111}In-Co(III) Janus: five mice, ^{67}Ga-Co(III) Janus: three mice] or the pretargeted antibody [^{111}In-Co(III) Janus: five mice, ^{67}Ga-Co(III) Janus: three mice] was omitted.

TABLE 1
Tumor-to-Organ Ratios of ^{111}In- and ^{67}Ga-Cobalt (III) Janus in Mice with Tumors

	WC 3A11 50 μG 20 hr HTr2IT (Co) babe 21 hr In-111 (Co) Janus			WC 3A1150 μG 20 hr HTr2IT (Co) babe 21 hr ^{67}Ga (Co) Janus		
n = 3	% Dose/g	s.d.	T/O Ratio	% Dose/g	s.d.	T/O Ratio
Blood	0.67	0.08	11.06	0.70	0.26	12.82
Heart	1.01	0.07	7.32	0.92	0.22	9.32
Lungs	2.41	0.34	3.08	1.90	0.26	4.43
Liver	1.66	0.47	4.59	2.93	1.91	3.61
Spleen	0.51	0.01	14.53	0.38	0.14	23.66
Kidneys	7.62	1.22	0.98	8.16	2.61	1.09
Tumor	7.36	1.00	1.00	8.44	1.15	1.00
Muscle	0.86	0.48	10.30	0.38	0.21	27.60
Bone	1.12	0.18	6.64	1.01	0.42	9.44
Skin	1.33	0.14	5.58	0.52	0.27	19.08
Gut	3.68	0.57	2.01	7.67	1.80	1.13

RESULTS

In Vitro

The K_A of WC3A11 and ^{57}Co-Co(III) ½ Janusol = 2.6 ± [0.1(s.d.)] × 10^8 (n = 6, r^2 = 0.93), and ^{111}In-In(III) ½ Janusol = 2.9 ± [1.5(s.d.)] × 10^7, (n = 6, r^2 = 0.93). As expected the highest affinity was shown for ^{57}Co-Co(III) ½ Janusol, the monovalent hapten with a structure closest to that of the original antigen. The tenfold decrease in K_A when the metal ion was changed to In(III) in ½ Janusol was small compared to In(III)benzyl EDTA with no side chain, which had no measurable binding to WC3A11. It was not possible to obtain a reliable K_A value by equilibrium dialysis for ^{57}Co-Co(III) Janus or ^{111}In-In(III) Janus, since the data did not give a straight line on a Scatchard plot. This is expected for the binding of a bivalent hapten to a bivalent antibody.

Biological Half-life

The ^{111}In and ^{67}Ga-Co(III) Janus were both rapidly excreted ($T_{1/2_h}$ = 42 min; >93% excreted in 24 hr) from mice in the absence of antibody. The complex of both ^{111}In and ^{67}Ga-Co(III) Janus with WC3A11 was retained much longer ($T_{1/2_h}$~24 hr). The 24-hr retention of a mixture of 50 μg WC3A11 and ^{57}Co-, ^{111}In- and ^{67}Ga-Co(III) Janus ranged from 33% to 53%. When the chase was administered to pretargeted mice 1 hr before ^{111}In-Co(III) Janus, whole body retention fell from >85% to approximately 10%, 24 hr after pretargeted antibody (3 hr post-tracer).

Organ Distribution

The 3-hr organ and tumor distributions and tumor-to-organ ratios of ^{111}In- and ^{67}Ga-Co(III) Janus in tumor mice is shown in Table 1 and Figure 2. The tumor concentrations of ^{111}In-Co(III) Janus = 7.4 ± 1%/gm and ^{67}Ga-Co(III) Janus = 8.4 ± 1.2%/gm; significantly higher than that we obtained with monovalent haptens [1.4 ± 0.6%/gm: $p < 0.001$ (Student's unpaired t-test)] (*5*). However, there were no significant differences in the high tumor-to-organ ratios between these two studies (Fig. 3). The absolute tumor concentrations of bivalent hapten in the present study are equivalent to values we obtained (8.1 ± 1%/gm, n = 11) with ^{111}In chelate conjugates of nonspecific IgG at 20-hr postinjection in the same tumor mouse model (*18*). However, with directly labeled ^{111}In antibody, >85% injected dose remained at this time and the blood levels were higher than the tumor: T/B1 ratio = 0.7/1.

When Janus was given to pretargeted mice without the chase, liver uptake was equal to 35% (Fig. 2) whereas with monovalent hapten liver uptake was equal to 23 ± 4% (*5*). This suggested that bivalent Janus cross-linked circulating antibody, which was then more efficiently removed by the liver. The Janus tumor-to-organ ratios were all > 3:1 (tumor/blood > 10:1) except kidney and gut, the routes of excretion of the hapten (Fig. 3). Since the tumors

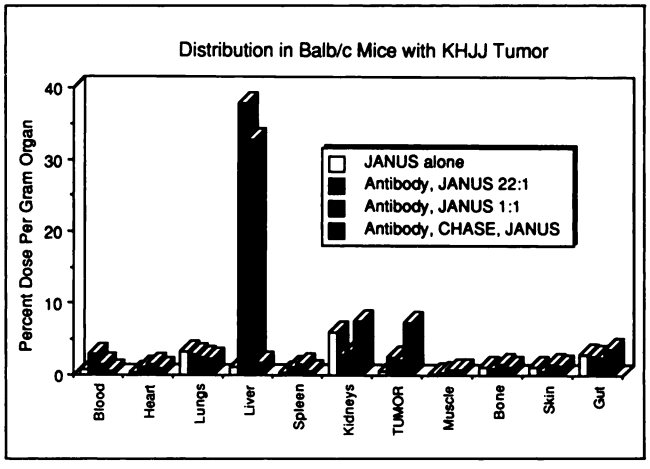

FIGURE 2. Three-hour organ distribution (percent injected dose per g) of ^{111}In-Co(III) Janus in mice with KHJJ tumors. Very low concentration in all organs and tumor of Janus alone. Much higher levels in animals pretargeted with WC3A11, especially liver due to cross-linking of circulating Mab. When blood is cleared with chase, liver uptake is greatly decreased and tumor concentration is increased.

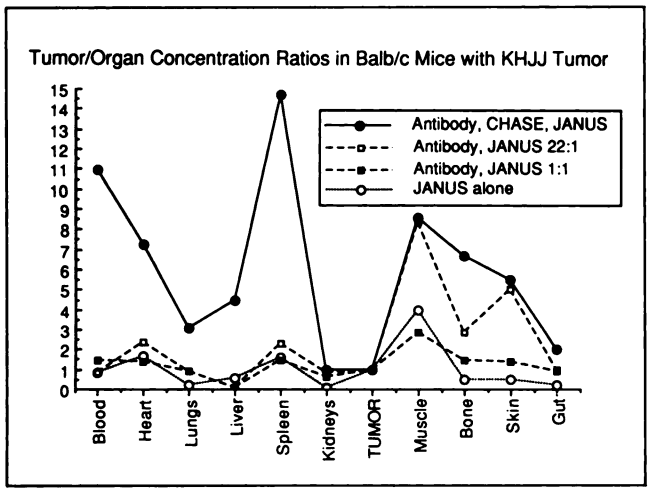

FIGURE 3. Tumor-to-organ ratios are greatly improved with the chase, especially tumor-to-liver and tumor-to-blood ratios. Tumor-to-kidney ratio is < 1 since it is the main route of excretion of Janus and the tumor-to-gut ratio is also low due to some excretion by this route.

weighed ~ 0.3–0.5 g, ~3%–4% of the injected dose was localized in the tumor. A major improvement over covalent ^{111}In chelate conjugates (*18,19*) was seen in the low nontumor tissue activity especially in the liver (Fig. 3). Total body retention at 3 hr was only ~10% compared to ~50% without the chase and >85% for chelate conjugates (*18,19*).

Tumor Mouse Images

The 3-hr images made with ^{111}In or ^{67}Ga-Co(III) Janus alone and with ^{111}In or ^{67}Ga-Co(III) Janus in pretargeted mice with and without chase are shown in Figure 4. With ^{111}In-Co(III) Janus alone (Fig. 4A), only ~5.2% of the injected dose remained at 3 hr. The tumor is not well seen and contained only ~0.6% of the counts by digital ROI analysis. With pretargeting (Fig. 4B), tumor uptake did not change and in addition there was a large background (~50% of the dose remaining; 0.8% in tumor). Note the large liver activity in Figure 4B due to cross-linking. With chase (Fig. 4C), the tumor stands out much better against the lower body background. Only ~10% of the dose remained in the whole body at the 3-hr imaging time, with greatly improved T/O ratios and image contrast. The tumor contained ~7% of the counts by ROI analysis. Note the low liver background in the chase image (Fig. 4C).

DISCUSSION

The high liver background seen in images made with ^{111}In antibody conjugates is made worse with second antibody chase (*18,19*). Chase given following administration of premixed antibody ^{111}In hapten complex, while lowering blood activity, does not significantly improve liver background (*20,21*); nor do metabolizable linkers offer much improvement so far (*22*). However, the three-step pretargeting method (*5,23*) which we have modified here, has produced a significant reduction in most organ background levels including the liver. Importantly for possible future radioimmunotherapy applications, whole body radiation burden was reduced by >70% over ^{111}In antibody conjugates.

The first pretargeting step was i.v. injection of antibody followed by a sufficient time interval for slow diffusion from blood through the extracellular fluid to the tumor target. It may take several days in humans to reach maximum target concentrations due to the slow pharmacokinetics of antibodies (*24*). Tumor uptake of nonspecific antibody in the present animal model occurred primarily because of the presence of relatively leaky capillaries. The second step required rapid blood clearance (minutes, compared to days for diffusion) of excess circulating nonradioactive antibody after localization in the target had occurred. It was necessary to do this with minimum reduction of target antibody. This was accomplished with antigen covalently bound to a slowly diffusible serum protein, either transferrin or nonspecific IgG. A minimum of four hapten molecules per molecule of protein was used to allow cross-linking and lattice formation in the plasma. The relatively large aggregates thus formed were rapidly removed from the blood by the RE cells of the liver, analogous to liver clearance of colloidal particles. Here, they were apparently sequestered in a site (probably intracellular), unavailable to the extracellular radiolabeled hapten. Excess unreacted chase remained predominantly within the vascular space and did not have time to diffuse into the target or other tissues in the 1 hr before the tracer was administered. In the final and third step, the desired tracer was given intravenously as a rapidly diffusible weakly binding monovalent, or strongly binding bivalent hapten complex.

For a bivalent molecule A-B, where both A and B are haptens, binding to an antibody site S may be described most simply, for the case where binding of the antibody to either hapten has no effect on the other. We write two

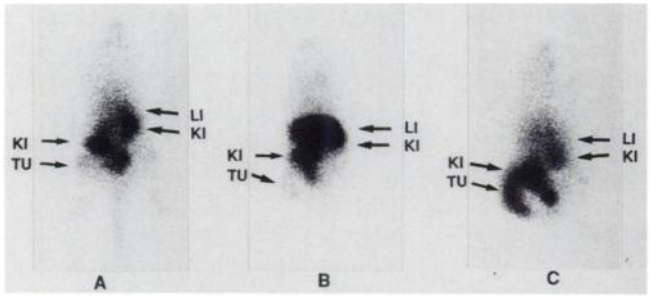

FIGURE 4. Three-hour 200k (100–500 μCi ^{111}In-Co(III) Janus) posterior pin-hole images of prone BALB/c mice with KHJJ tumors in the flank. (A) Janus alone; ~5.2% of the injected dose remaining. (B) Pretargeted but no chase; larger liver uptake, ~50% injected dose remaining. (C) Pretargeted with chase; tumor is now clearly visible and liver activity much decreased, ~7% injected dose remaining.

separate equilibrium constants, expressed in terms of the concentrations of *ends*:

$$K_A = \frac{[AS]}{[A][S]} \qquad \text{Eq. 1}$$

$$K_B = \frac{[BS]}{[B][S]} \qquad \text{Eq. 2}$$

The fraction of bivalent hapten bound by A is given by (*25*):

$$Q_A = \frac{[AS]}{[A] + [AS]} = \frac{K_A[S]}{1 + K_A[S]} \qquad \text{Eq. 3}$$

A similar function holds for Q_B, so the total fraction of hapten bound by either end is:

$$Q_{tot} = Q_A + Q_B = \frac{K_A[S]}{1 + K_A[S]} + \frac{K_B[S]}{1 + K_B[S]} \qquad \text{Eq. 4}$$

Thus, the fraction bound depends on both K_A and K_B. If these binding constants have very different values, the largest will dominate. When the two ends of the molecule are identical (A = B), then:

$$Q_{tot} = \frac{2K_A[S]}{1 + K_A[S]}, \qquad \text{Eq. 5}$$

and binding is twice what it would be for a monovalent hapten. In this case, the overall equilibrium constant is:

$$K_{tot} = \frac{\{[A - AS] + [SA - A]\}}{[A - A][S]} \qquad \text{Eq. 6}$$

If the concentration of a bivalent hapten is not expressed in terms of the ends, but rather in terms of moles bivalent hapten per liter, then the concentration of free bivalent hapten is half the concentration of ends, and another factor of two appears in the equilibrium constant, because [A-A] = [A]/2. Thus theoretically $K_{tot} = 4\ K_A$ if the ends behave independently.

If the hapten concentration is much larger than the antibody concentration, then it is unlikely that both ends of a bivalent hapten will be bound. Conversely, if the antibody concentration is much larger than the hapten concentration, and if the antibody site concentration [S] $\geq 1/K_A$ and [S] $\geq 1/K_B$, then bivalent binding becomes important. The limitation that antibody-hapten binding constants are seldom $> 10^9$ can be alleviated in some circumstances by the binding of two antibodies to a single, bivalent hapten. For example, Mab WC3A11 binds Co(III) ½ Janusol chelates with an aliphatic hydrocarbon chain in the para position, with $K_A \approx 2.6 \pm [0.1\ (s.d.)] \times 10^8$. The injection of 10 mg WC3A11 (or an equivalent amount of a conjugate with an antitumor Mab) will lead to a concentration of chelate-binding Mab sites $\approx 4.3 \times 10^{-8}\ M$ in the human circulation. If a small amount of radiolabeled Janus were to be added, most of it would bind two molecules of WC3A11. A simple equilibrium calculation (see Fig. 5) reveals that since Janus is bivalent, $\approx 0.2\%$ would not be bound by $\approx 4.4 \times 10^{-8}\ M$ WC3A11 sites ($\{1 - Q\} = \{1 + 2K_A\ [sites] + K_A^2\ [sites]^2\}^{-1}$); for a monovalent hapten, $\approx 5\%$ would not be bound $\{1 - Q\} = \{1 + K_A\ [sites]\}^{-1}$).

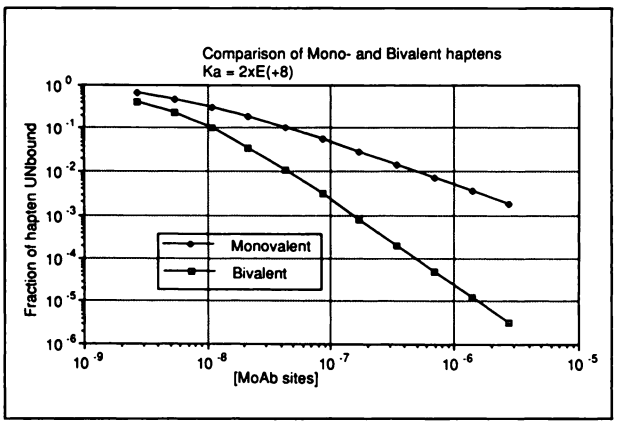

FIGURE 5. Equilibrium considerations predict enhanced binding of bivalent over monovalent haptens. This advantage increases with increasing concentrations of antibody as shown in the graph plotted from calculated values of K_A.

Now consider the rate of escape of radiolabeled Janus from a region of high WC3A11 concentration, e.g., a tumor. The essence of pretargeted tumor localization deals with the rate of clearance of radiolabel from the body (which should be fast) relative to the rate of clearance from the tumor (which should be as slow as possible). The rate of clearance depends directly on the fraction of radiolabel that is not bound. If the concentration of WC3A11 in a tumor were $4 \times 10^{-8}\ M$, while its concentration elsewhere was much less, the rate of loss of radiolabel from the tumor would be ≈20× slower for a bivalent hapten than a monovalent one. While we have not measured these washout rates directly, if we assume the same WC3A11 tumor concentrations in both our mono and bivalent hapten experiments [50 μg were injected in both (*5,6*)], then the ratio of the 3-hr tumor concentrations [7.36%/gm bivalent]/[1.4%/gm monovalent] = 5.26. This is in close agreement with the calculated theoretical factor of 5. If the targets are malignant cells in the circulation, an anticancer antibody like Lym-1 (anti-B cell lymphoma) is likely to have an effective concentration on the cell surface that is much greater than the concentration of Mab in blood, and the bivalent hapten's advantage will be magnified. On the other hand, it will be difficult to achieve such a concentration throughout a solid tumor. However, in some solid tumors the Mab accumulates in microscopic pockets, which after chase, might produce a similar result (*26*).

Le Doussal et al. have recently reported improved target-to-background ratios in vitro (lymphocytes) and in vivo (spleen) with a dual specificity Mab conjugate (DSC) and bivalent hapten (*7*). The Mab CY34 anti-Lyb8.2 mouse B cell antigen used in these experiments was rapidly inter-

nalized so pretargeting in vivo was limited to 10 min. Much higher spleen localization was noted with bivalent hapten and was attributed to "enhanced" affinity of cell-bound DSC for bivalent haptens.

This "enhanced" affinity was explained by the more stable configuration of cell bound bivalent hapten-conjugate complex than the bivalent hapten-conjugate complex in solution in the circulation. The cell-bound complex included: one bivalent hapten, two $F(ab')_2$-Fab conjugates, four antigens and the cell wall. The completion of such a stable "ring" was not possible in the circulation since the conjugate consisted of divalent anti-Lyb8.2 allelic anti-B cell antigen [$F(Ab')_2$] covalently linked to monovalent antihapten (anti 2,4 dinitrophenol) Fab. In solution, in plasma, bivalent hapten could bind only two bifunctional antibody conjugates through the two Fab moieties, in an open, less stable linear dimer configuration. One apparent advantage of this "enhanced" affinity of bivalent hapten for cell-bound conjugate was that a chase was not necessary to lower the concentration of circulating complex, since bivalent hapten bound more strongly to the solid phase complex (stable "ring") in the target. More weakly bound circulating bivalent hapten was rapidly excreted through the kidneys.

This technique has now been successfully extended to imaging human melanoma in nude mice (*27*) and to selectively targeting double-antigen-positive mouse B cells in vivo, using a cocktail of two specific Mab conjugates and one asymmetric bivalent hapten (*28*). In the latter system, only cells expressing both antigens can bind both simultaneously administered conjugates to form the stable ring configuration with the asymmetric bivalent hapten. To cells with only one antigen and thus binding only one of the two conjugates, the asymmetric bivalent hapten is functionally monovalent: affinity enhancement (ring formation) cannot occur, and the asymmetric bivalent hapten is rapidly excreted. The use of such asymmetric bivalent haptens, together with matched (antihapten, anticell) antibody conjugates, is proposed as a general method for increasing the in vivo specificity of immunoscintigraphy and radioimmunotherapy.

In addition to the mechanism proposed by Le Doussal et al., which requires cell binding of antibody for enhanced affinity, our results with nonspecific bivalent antihapten antibody show that cell binding is not an absolute requirement for preferential tumor uptake. Electron microscope studies have shown formation of ring-shaped complexes containing predominantly two bivalent haptens and two bivalent antihapten IgG_1 monoclonal antibodies (*29*). Equilibrium considerations (see above) predict enhanced binding of bivalent over monovalent haptens, an advantage that increases at higher antibody concentrations (Fig. 5). Such a concentration gradient between tumor (high) and blood (low) exists one hr after the chase in our tumor mouse model.

A further possible use of a bivalent hapten, important for therapy, is to induce internalization of a bispecific antibody by cross-linking it on a cell surface. A bispecific antibody could first bind by its antitumor arm to a cell-surface antigen and then, after administration of a bivalent hapten, be cross-linked to another bispecific antibody, triggering internalization by the target cell (*30,31*).

Certain physiological properties of the radiolabeled haptens, whether monovalent or bivalent, are important to ensure fast elimination from the body. Anderson et al. (*32*) found that modifications in ligand structure greatly altered the observed biodistribution in a bispecific antibody system, ECHO37.2, derived from fusion of the CHA255 cell line and an anti-CEA Mab-producing cell line CEM231. For early target uptake, the labeled hapten must be relatively small and rapidly diffusible throughout the extra-cellular space in order to reach the tumor quickly. It should also be relatively hydrophilic to decrease nonspecific binding and promote quick clearance by glomerular filtration via the kidneys. As the lipophilicity of the hapten increases, excretion through the liver and biliary system occurs, which may produce confusing gut activity on the scan (*24*). The DNP biderivatized hapten of Le Doussal et al. had detrimental hydrophobic properties (*7*), compared to the more ideal di-DTPA TL hapten (*7,27*). The ^{111}In-Co(III) Janus also fulfilled the above criteria for pretargeted imaging.

The development of bispecific antibodies that could bind both a chelate hapten and a tumor antigen is now undergoing active investigation (*33*). Either hybrid antibodies (*34,35*) or antibody conjugates (*36*) could be used for this application. Improved distribution in the nude mouse colon cancer model has been obtained using two Fab' fragments coupled at the SH groups via a heterobifunctional cross-linker (*33*). One Fab was specific for the radiolabeled chelate, the other for CEA. Stickney et al. have reported improved results in nine patients with colon cancer using this conjugate (*37*). In this study, carrier bispecific Mab was injected together with the hapten.

Other strategies employing pretargeting have been described (*38*). Avidin and biotin, have affinities much higher than antibodies (10^{15}), and Hnatowich et al. and others have demonstrated improved distribution in mice with this system (*39,40*). Paganelli et al. have recently reported excellent human colon cancer images in 20 patients with 1 mg of pretargeted biotinylated Mab followed by Avidin and then ^{111}In biotin-chelate conjugate (*41*). A pharmacokinetic analysis of pretargeted bispecific and enzyme-conjugated antibodies (*42*) by Yuan et al. (*43*) shows the theoretical value of background reduction.

In summary, the pretargeting method gives absolute tumor concentrations of radioactivity that produce excellent mouse tumor images and are also quantitatively high enough for possible future radioimmunotherapy. The novel feature is the greatly reduced background activity in normal tissues. This is critical for increased image contrast in radioimmunoscintigraphy of small tumors and reduc-

tion of bone marrow radiation, currently the major limiting factor in radioimmunotherapy with covalently radiolabeled monoclonal antibodies.

ACKNOWLEDGMENTS

These studies were supported in part by a grant from the Veterans Administration (DAG) and PHS grants number CA 28343, CA 48282 (DAG) and CA 16861 (CFM). Preliminary oral presentation of this work was made at the 13th annual Western Regional Society of Nuclear Medicine meeting, Seattle, WA, Oct. 13–16, 1988.

REFERENCES

1. Halpern SE, Hagen PL, Garver PR, et al. Stability, characterization and kinetics of ^{111}In-labeled antitumor antibodies in normal animals and nude mouse-human tumor models. *Cancer Res* 1983;43:5347–5355.
2. Hnatowitch DJ, Griffin TW, Kosciuczyk C, et al. Pharmacokinetics of an ^{111}In-labeled monoclonal antibody in cancer patients. *J Nucl Med* 1985; 26:849–858.
3. Chatal JF, Saccavini JC, Fumoleau P, et al. Immuno-scintigraphy of colon carcinoma. *J Nucl Med* 1984;25:307–314.
4. Reardon DT, Meares CF, Goodwin DA, et al. Antibodies against metal chelates. *Nature* 1985;316:265–268.
5. Goodwin DA, Meares CF, McCall MJ, McTigue M, Chaovapong W. Pretargeted immunoscintigraphy of murine tumors with indium-111-labeled bifunctional haptens. *J Nucl Med* 1988;29:226–234.
6. Goodwin DA, Meares CF, McCall MJ, Chaovapong W, McTigue M, Diamante CI. Pretargeted immunoscintigraphy with In-111, Ga-67 and Ga-68 labeled bivalent ("Janus") haptens [Abstract]. *J Clin Nucl Med* 1988; 13:9Sp10.
7. Le Doussal J-M, Martin M, Gautherot E, Delaage M, Barbet J. In vitro and in vivo targeting of radiolabeled monovalent and divalent haptens with dual specificity monoclonal antibody conjugates: enhanced divalent hapten affinity for cell-bound antibody conjugate. *J Nucl Med* 1989;30: 1358–1366.
8. Karush F. Multivalent binding and functional affinity. *Contemp Top Mol Immunol* 1976;5:217.
9. Meares CF, McCall MJ, Reardan DT, Goodwin DA, Diamanti CI, McTigue M. Conjugation of antibodies with bifunctional chelating agents: isothiocyanate and bromoacetamide reagents, methods of analysis, and subsequent addition of metal ions. *Anal Biochem* 1984;142:68–78.
10. Mukkala VM, Mikola H, Hemmila I. The synthesis and use of activated N-benzyl derivatives of diethylenetriaminetetraacetic acids: alternative reagents for labelling of antibodies with metal ions. *Anal Biochem* 1989; 176:319–325.
11. DeRiemer LH, Meares CF, Goodwin DA, et al. BLEDTA II: Synthesis of a new tumor-visualizing derivtive of Co(III) bleomycin. *J Labeled Compds* 1981;18:1517–1534.
12. Kramer SP, Goodman LE, Dorfman H, et al. Enzyme alterable alkylating agents. VI. Synthesis, chemical properties, toxicities, and clinical trial of haloacetates and haloacetamides containing enzyme susceptible bonds. *J Natl Cancer Inst* 1963;31:297–326.
13. Udenfriend S, Stein S, Bohlen P, et al. Fluorescamine; a reagent for assay of amino acids, peptides, proteins and primary amino acids in the picomolar range. *Science* 1972;178:871–872.
14. Ellman GL. Tissue sulfhydryl groups. *Arch Bioch Biophys* 1959;82:70–77.
15. Penefsky HS. A centrifuged-column procedure for the measurement of ligand binding by beef heart F1. In: Fleischer S, ed. *Methods in enzymology*, volume 56. New York: Academic Press; 1979: Part G, 527–530.
16. Lowry OH, Roseborough NJ, Farr I, et al. Protein measurement with the Folin phenol reagent. *J Biol. Chem* 1951;193:265.
17. Goodwin DA, Sundberg MW, Diamanti CI, Meares CF. ^{111}In radiopharmaceuticals in cancer localization. In: Thomas P, Haynie, ed. *Proceedings of 18th annual clinical conference 1973. Radiological and Other Biophysical Methods in Tumor Diagnosis.* MD Anderson Hospital and Tumor Institute. Houston, Texas: Yearbook Medical Publishers; 1975:57–88.
18. Goodwin DA, Meares CF, Diamanti CI, et al. Use of specific antibody for rapid clearance of circulating blood background from radiolabeled tumor imaging proteins. *Eur J Nucl Med* 1984;9:209–215.
19. Goodwin DA, Meares CF, McCall MJ, et al. Chelate conjugates of monoclonal antibodies for imaging lymphoid structures in the mouse. *J Nucl Med* 1985;26:493–502.
20. Goodwin DA, Meares CF, McTigue M, David GS. Monoclonal antibody hapten radiopharmaceutical delivery. *Nucl Med Commun* 1986;7: 569–580.
21. Goodwin DA, Meares CF, David GF, et al. Monoclonal antibodies as reversible equilibrium carriers of radiopharmaceuticals. *Int J Nucl Med Biol* 1986;13:383–391.
22. Haseman MK, Goodwin DA, Meares CF, et al. Metabolizable ^{111}In chelate conjugated anti-idiotype monoclonal antibody for radioimmunodetection of lymphoma in mice. *Eur J Nucl Med* 1986;12:455–460.
23. Goodwin DA, Meares CF, McTigue M, McCall MJ, David GS. Rapid localization of hapten in sites containing previously administered antibody for immunoscintigraphy with short half-life tracers [Abstract]. *J Nucl Med* 1986;27:959.
24. Goodwin DA. Editorial. Pharmacokinetics and antibodies. *J Nucl Med* 1987;28:1358–1362.
25. Cantor CR, Schimmel OR. *Biophysical chemistry, volume III.* San Francisco: W. H. Freeman & Co., 1980:856–857.
26. Tilgen W, Matzku S, Kaufman I, et al. Modulation of melanoma associated antigens by monoclonal antibodies as visualized by radioimmunoelectron microscopy and radioantibody binding assay. *Arch Derm Res* 1987;279: (suppl I)S116–126.
27. Le Doussal J-M, Grouaz-Guyon A, Martin M, Gautherot E, Delaage M, Barbet J. Targeting of indium-111-labeled bivalent hapten to human melanoma mediated by specific monoclonal antibody conjugates: imaging of tumors hosted in nude mice. *Cancer Res* 1990;50:3445–3452.
28. Le Doussal J-M, Gautherot E, Martin M, Barbet J, Delaage M. Enhanced in vivo targeting of an asymmetric bivalent hapten to double-antigen-positive mouse B cells with monoclonal antibody conjugate cocktails. *J of Immunol* 1991;146:169–175.
29. Phillips ML, Oi VT, Schumaker VN. Electron microscopic study of ring-shaped, bivalent hapten, bivalent antidansyl monoclonal antibody complexes with identical variable domains but IgG_1, IgG_{2a} and IgG_{2b} constant domains. *Mol Immun* 1990;27:181–190.
30. Matzku S, Broecker E, Bruggen J, Dippold W, Tilgen W. Modes of binding and internalization of monoclonal antibodies to human melanoma cell lines. *Cancer Res* 1986;46:3848–3854.
31. Matzku S, Tilgen W, Kalthoff H, Schmiegel W, Broecker E. Dynamics of antibody transport and internalization. *Int J Cancer* 1988;2(suppl):11–14.
32. Anderson LD, Meyer DL, Battersby TR, et al. Optimization of ligand structure for imaging with a bifunctional antibody (Abstract). *J Nucl Med* 1988;29:835.
33. Frincke JM, Halpern SE, Chang C-H, et al. Radioimmunodetection (RID) approach using an ^{111}In hapten (H) monoclonal antibody (MoAb): studies in the nude mouse-human colon tumor mode [Abstract]. *J Nucl Med* 1987;28:711.
34. Suresh MR, Cuello AC, Milstein C. Advantages of bispecific hybridomas in one-step immunocytochemistry and immunoassays. *Proc Natl Acad Sci USA* 1986;83:7989–7993.
35. Bosslet K, Stienstraesser A, Hermentin P, et al. Generation of bispecific monoclonal antibodies for two phase radioimmunotherapy. *Br J Cancer* 1991;63:681–686.
36. Brennan M, Davison PF, Paulus H. Preparation of bispecific antibodies by chemical recombination of monoclonal immunoglobulin G_1 fragments. *Science* 1985;229:81–83.
37. Stickney DR, Frincke JM, Slater JB, Ahlem CN, Merchant B, Slater JM. Bifunctional antibody clinical trials: a new method for cancer imaging and therapy [Abstract]. *Clin Nucl Med* 1987;12,P16.
38. Goodwin DA. Strategies for antibody targeting. *Antibody, Immunoconj Radiopharm* 1991;4:427–434.
39. Hnatowitch DJ, Virzi F, Ruskovsky M. Investigations of avidin and biotin for imaging applications (Abstract). *J Nucl Med* 1987;28:560.
40. Goodwin DA, Meares CF, McCall MJ, McTigue M. An avidin biotin chelate system for imagiong tumors (Abstract). *J Nucl Med* 1987;28:722.
41. Paganelli G, Magnani P, Zito F et al. Three-step monoclonal antibody tumor targeting in carcinoembryonic antigen-positive patients. *Cancer Res* 1991;51:5960–5966.
42. Senter PD. Activation of prodrugs by antibody-enzyme conjuugates: a new approach to cancer therapy. *FASEB J* 1990;4:188–193.
43. Yuan F, Baxter LT, Jain RK. Pharmacokinetic analysis of two-step approaches using bifunctional and enzyme-conjugated antibodies. *Cancer Res* 1991;51:3119–3130.